The ACPI demonstration project, Element 1: Initializing the Coupled Model from Observed Conditions

David W. Pierce and Tim P. Barnett

Climate Research Division, Scripps Institution of Oceanography
La Jolla, California

Detlef Stammer

Center for Observations, Modeling, and Prediction at Scripps Institution of Oceanography
La Jolla, California

Albert Semtner and Robin Tokmakian

Naval Postgraduate School
Monterey, California

Mathew Maltrud

Los Alamos National Laboratory
Los Alamos, New Mexico

Tue Nov 6 14:39:41 PST 2001

ABSTRACT

A problem for climate change studies with coupled ocean-atmosphere models has been how to incorporate observed initial conditions into the ocean, which holds most of the "memory" of anthropogenic forcing effects. The first difficulty is that there are no comprehensive three-dimensional observations of the current ocean temperature (T) and salinity (S) fields to initialize to. The second problem is that directly imposing observed T and S into the model would likely result in rapid drift back to the model climatology, with the corresponding loss of the observed information. This problem is particularly acute with anthropogenic forcing scenarios; since the forcing is secularly increasing, a monotonic climate response is probable, which would be hard to distinguish from drift. For this reason, anthropogenic forcing scenarios typically initialize future runs by starting with pre-industrial conditions, but this $\sim$130 yr spinup imposes substantial overhead if only a few decades of predictions are desired. Also, if the future climate depends on the details of the present climate, then initializing the model to observations may provide more accurate forecasts. A technique to address these problems is presented here. In lieu of observed T and S, assimilated ocean data from an adjoint model were used. To reduce the problem of model drift, an anomaly coupling scheme was devised. This consists of letting the model's climatological (pre-industrial) oceanic and atmospheric heat transports balance each other, while adding on the (much smaller) anthropogenic changes in heat tranport since the pre-industrial era as anomalies. It is shown that this technique works because the anomalous (due to anthropogenic forcing) temperature fields in the model and observations are similar in both pattern and magnitude. The result is model drift of no more than 0.2 C over 50 years, which is significantly smaller than the forced response of 1.0 C. The ensemble of runs with assimilated initial conditions is then compared to a set spun up from pre-industrial conditions; no systematic differences were found. This is likely another manifestation of the similarity between the model and observations; a model with a worse representation of the late 20th century climate might show significant differences if initialized in this way.

1. Introduction

The Accelerated Climate Prediction Initiative (ACPI) is a DOE-sponsored project to determine the effects of anthropogenic forcing on the world's climate. Clearly this is a question with broad scope, so the full ACPI project as envisioned could easily consume a great deal of resources. Rather than fund the entire project at once, it was determined that implementing a more limited, proof-of-concept experiment would be valuable. This led to the proposal of the pilot-ACPI project (also called the ACPI demonstration project), which would use the same techniques and machinery as the full ACPI project, but applied to a more limited set of final questions. This pilot project would encounter the same difficulties expected in the full ACPI project, but because of its smaller size, the problems would be more tractable. Solutions to the problems found in the pilot project could then be applied to the full ACPI project, enabling the latter to progress more smoothly.

The objective chosen for the pilot-ACPI project was a demonstration of "end-to-end" prediction of water resources in the western U.S. over the period 1995 to 2050. By "end-to-end", it was meant that the project would start with the observed climate state at the end of the twentieth century, take into account projections of anthropogenic forcing (primarily CO_2 and sulfates) for the next 50 years, and conclude with detailed predictions of hydrological changes in the western states expected by the year 2050. Some examples of the anticipated final predictions include snowpack depth, snow coverage, and time-dependent runoff. This information could then be used by water managers to determine if there were potentially any problems with water supply availability in coming decades.

The pilot-ACPI project consisted of three specific elements to achieve this end-to-end predictive capability:

1. Initializing the coupled ocean-atmosphere general circulation model (O/A GCM) with observed conditions.

2. Running ensembles of the coupled model from the initial condition to year 2050 and beyond using "business as usual" (BAU) anthropogenic forcing scenarios.

3. Downscaling the global model results using high resolution regional atmospheric, hydrological, and runoff models to give impacts on water resources.

The first objective of this note is to describe the technique used to accomplish element 1, the initialization of the coupled O/A GCM with observed conditions. The second objective is to address, in a quantitative way, whether initializing to observations results in different climate forecasts than obtained from a spin-up run starting with pre-industrial conditions.

This note is laid out as follows. The O/A GCM used for these experiments will be briefly described in section 2. There were three main difficulties encountered during element 1; the first problem was the lack of comprehensive three-dimensional observations of the oceanic temperature (T) and salinity (S) fields, which we addressed by using an assimilated ocean data product as a surrogate for observations (section 3). The second problem (deemed the most scientifically difficult) was how to introduce the observed T and S fields into the coupled model without having drift that would obscure the signals of interest. An anomaly coupling scheme was used, as described in section 4. The third problem was how to initialize the model to a near-neutral state for interdecadal and interannual variability (those being not of direct interest in this project) despite initializing to year $\sim$1997, which was an unusually strong El Nino year. This problem is described in section 5. After the completion of pilot ACPI element 2, we then evaluated whether the new initialization condition made any difference to the climate (section 6); we found that it did not, although with some important caveats. The note concludes with a discussion of the scientific questions left unanswered by the pilot project (section 7).

2. The parallel coupled model

This work used the Parallel Coupled Model (PCM), version 1 (Washington et al. 2000). PCM is a state of the art, fully coupled ocean-atmosphere general circulation model (for more information see http://www.cgd.ucar.edu/pcm).

The atmospheric component of the PCM is the CCM3 atmospheric general circulation model (Kiehl et al. 1998), a spectral model used here at T42 resolution (equivalent to

about 280 by 280 km grid spacing). CCM3 includes a land surface model that accounts for soil moisture and vegetation types, as well as a simplified runoff scheme. A hybrid sigma coordinate scheme with 18 layers is used in the vertical, which allows terrain-following coordinates near the surface but segues to pressure levels higher in the air column.

The ocean component of PCM is the Parallel Ocean Program (POP; Smith et al. 1992, Dukowicz and Smith 1994), used here at a horizontal resolution of 384 by 288 (roughly 2/3° resolution), with 32 vertical levels. The vertical levels are clustered near the surface to improve resolution of the important surface mixing processes. A displaced-pole grid is used in the northern hemisphere to eliminate the problem of convergence of the meridians in the Arctic Ocean.

A dynamic-thermodynamic sea-ice model based on Zhang and Hibler (1997) is included, with an elastic-viscous-plastic rheology for computational efficiency (Hunke and Dukowicz 1997). The ice model is formulated on its own grid, which has a total of 320 by 640 gridpoints. The grid only covers the polar regions, and points are distributed approximately equally between the northern and southern hemispheres (i.e., each hemisphere is covered by a grid of about 320x320 points), giving a physical grid spacing of roughly 27 km.

3. The assimilated ocean data set

An objective of the pilot-ACPI project was to start with the best possible estimate of the actual climate state in the late twentieth century. This requirement was imposed because the warming the climate system has already experienced by the year 2000 might have an influence on the climate's later evolution. Ignoring this earlier warming is often referred to as the "cold start" problem (Hasselmann et al. 1993).

It is generally assumed, at least tacitly, that starting with the correct, anthropogenically warmed climate of the late twentieth century is important to predictions of future climate. This can be seen by the universality with which future climate change scenarios do *not* start out running in the late twentieth century, but rather in the late nineteenth century (see Schneider 1996 for further discussions of this issue). The PCM historical scenarios, for

example, start in 1870 (Washington et al. 2000). Atmospheric values of CO_2 are then gradually ramped up over the next 130 years to current values, resulting in a climate in the 1990s that is demonstrably warmer than the 1870 climate. If the objective were simply to forecast future climate change, it would be a waste of computer time to calculate the 1870 to 1995 change if it had no effect on the future predictions. Also, any errors in specifying historical forcing will accumulate during the spinup run to give an incorrect specification of today's climate.

The pilot-ACPI project chose to address the cold-start problem by initializing the coupled model to conditions appropriate to the late 20th century. However, we did *not* simply spin the coupled model up by starting in 1870 and ramping CO_2 and sulfate concentrations up to 1995 values. Rather, the model was initialized to the observed climate state. There were two reasons for this:

1. Going from 1870 to 1999 is a 130 year spinup, a large computer time overhead when the goal is to integrate only 50 years into the future.

2. If the future climate depends on the detailed representation of the late 20th century climate, then accurate forecasts require accurate initial conditions, and it can be supposed that observations provide a more accurate estimate of these conditions than a model spinup run forced by somewhat uncertain pollutant emissions.

An evaluation of the latter point is presented in section 6.

Most of the climate's "memory" of previous anthropogenic forcing resides in the ocean, specifically in an increase in the ocean's heat content (possibly with associated changes in the circulation), since the heat capacity of the ocean is so much greater than that of the atmosphere and cryosphere (Levitus et al. 2000). Changes in glaciers might also be of practical importance for ecosystems or sea level, but since the PCM has no dynamic glacier model it is a moot point for our purposes. Therefore, initializing to the correct climate state devolves to initializing to the correct ocean state.

The problem is that there are no systematic three dimensional observations of ocean T

and S to initialize to. In view of this lack, we used an assimilated ocean data product to provide T and S. We used the output of ECCO ocean state estimation project (Stammer et al. 1997; http://www.ecco.ucsd.edu), which assimilates observed sea surface height altimetry, NCEP surface forcing fields (heat, freshwater, and momentum), and the three-dimensional Levitus T and S fields into a full primitive equation oceanic GCM.

The ECCO project uses the MIT ocean model (Marshall et al. 1997a; Marshall et al. 1997b; Adcroft et al. 1997) at a 2x2 degree global resolution, and covers the period 1992 to 1997. The GCM is run in adjoint mode so that the T, S, and the forcing fields are adjusted until the observed and modeled data agree (subject to the constraints imposed by observational uncertainty and ocean physics). The final output is a set of correction fields that are applied to the NCEP forcing, as well as full three-dimensional fields of oceanic T and S. We used the latter to initialize the coupled model (our initialization technique is described in the next section).

An example of the correction obtained by the assimilation is given in Fig. 1. The top panel shows the original data from the NCEP analysis. The large positive values (heat flux out of the ocean) in the western boundary currents in winter can easily be seen, as well as the negative values (heat into the ocean) in the equatorial cold tongue. The middle panel shows the corrections to the NCEP data that the assimilation determines must be made in order for the surface forcing to be in agreement with the TOPEX/Poseidon data. The sense of the corrections is such that they must be subtracted from the original field. The final field after correction is shown in the bottom panel.

It can be seen in the middle panel that the greatest corrections are clustered in three areas: the Pacific equatorial cold tongue (particularly the upwelling region off Peru), and the two northern hemisphere regions where the western boundary currents separate from the coast. It is intuitively plausible that the NCEP surface fluxes might be especially bad in these regions. In the cold tongue, the exact surface heat flux depends on the detailed vertical structure of the ocean (poorly resolved by the NCEP model) as well as the systematic effects of local stratus clouds, which are not well represented in the model from which the

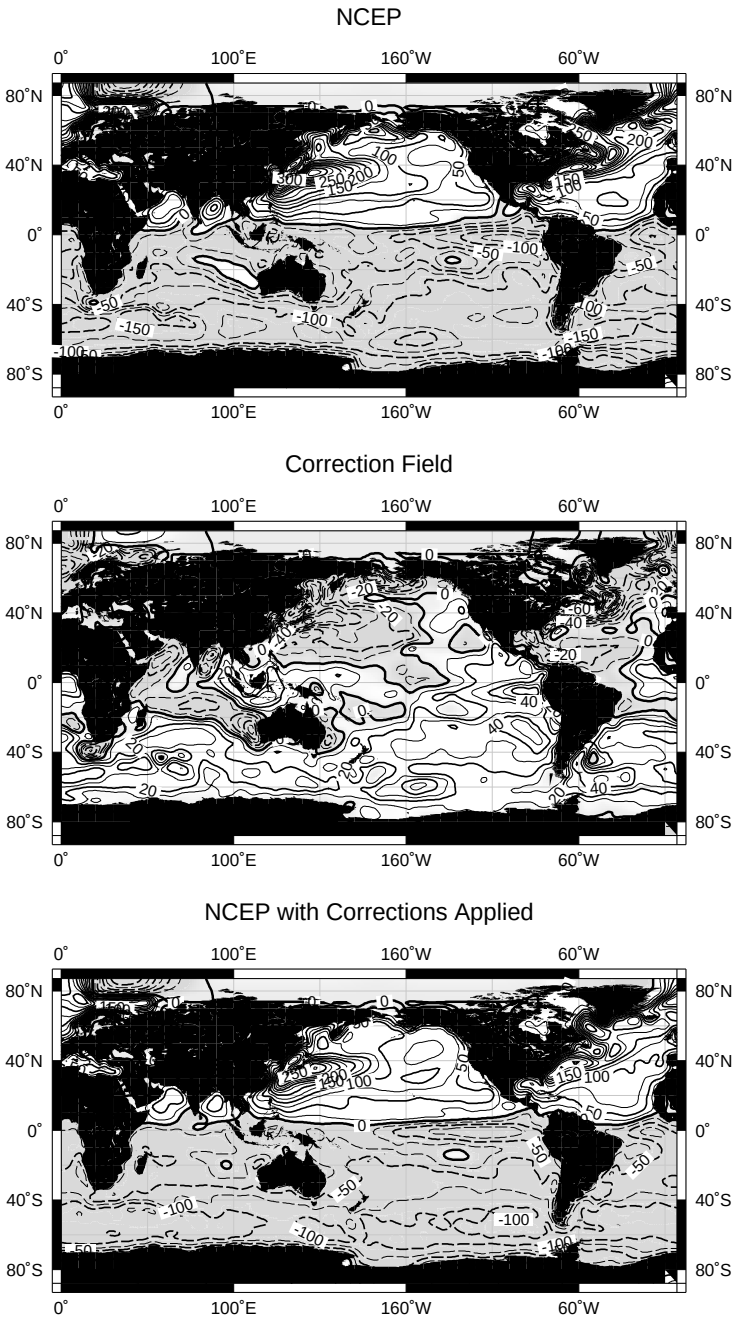

Figure 1: Net surface heat flux (W/m**2) during DJF. Top: the original NCEP data. Middle: the correction field. Bottom: the final, corrected field after the assimilation procedure. Negative values are shaded.

NCEP surface fluxes are ultimately derived. Similarly, the details of the separation of the western boundary currents are typically difficult for models to achieve.

In summary, a basic objective of the pilot-ACPI project was to start the coupled model from observed initial conditions. Given the lack of comprehensive three-dimensional observations, this was accomplished by using an assimilated ocean data set as a surrogate for observed conditions. (In later sections, the assimilated data will be referred to as the "observed" data.) An evaluation of the necessity for this basic objective is presented in section 6.

4. Coupled model initialization

Given the three-dimensional ocean data from the assimilation run, the next task was to incorporate these into the full PCM. The difficulty with this step is that mismatches between the implied heat transport of the model and observations (i.e., the assimilated data set) will cause the model's temperature to drift. Since the signal of interest is due to anthropogenic forcing, which itself is projected to undergo a secular increase over the period 1995-2050, any model temperature drift will mimic the secular forcing signal, potentially obscuring the forced response. It is therefore important to reduce the model drift as much as possible. In particular, it is necessary to have considerably less temperature drift than forced response if the results are to be interpreted as coming from the forcing instead of the drift.

a. Origin of the model drift

The origin of the temperature drift can be understood as follows. In an equilibriated model run, the oceanic and atmospheric heat transport must match, in the sense that wherever the ocean is carrying heat to the surface, the atmosphere must be carrying the same amount of heat away from that location. Any change in the (divergence of the) oceanic heat transport requires a corresponding change in the atmospheric heat transport. Potentially associated with this atmospheric change are alterations in surface wind stress, which in turn affect the ocean's heat transport. The result is model drift to a new equilibrium state where the ocean and atmosphere heat transports are again in balance.

Unfortunately, the heat transport field H is a difficult variable to work with, and there are no comprehensive global observations of it available to compare to. Therefore, we assume H to be a function of time expressed through the T and S fields: $H(\vec{\mathbf{x}}, t) = H(T(\vec{\mathbf{x}}, t), S(\vec{\mathbf{x}}, t))$. The motivation for this assumption is that the T and S fields determine the density and velocity fields (to a good approximation), and the T and velocity fields then determine H. This assumption is key to what follows since there exist reasonable observations of T and S to compare to, and the data assimilation scheme described in section 3 outputs these fields directly. Our later manipulations will be based exclusively on the T and S fields, although the motivation arises from considerations of the heat transport. The quality of the assumption relating H to T and S in the model context will be checked in section 4d.

Putting observed ocean T and S (and therefore, an implied H) directly into the ocean component of an equilibrated model run will result in substantial model drift, since the heat transport implied by the observed fields is unlikely to be identical to the heat transport of the model fields. In fact, if the model's climate has only one stable state (or only one state under small perturbations), then the model is guaranteed to eventually drift back to the original equilibrated condition, resulting in total loss of information from the observed T and S fields. As a practical matter, the goal is to have much less model drift than forced response over the period of interest.

Several methods were considered to address this problem. An attempt was first made to simply put the observed T and S fields directly into the model. The hope was that the inevitable model drift would be small compared to the forced signal over the relatively brief timescale of interest ($\sim$50 years). It turned out that the model drift was substantial, and a more sophisticated procedure would have to be used.

Various flux correction schemes were also considered. The philosophy of these is to put the observed ocean T and S fields into the coupled model, then diagnose the surface heat flux mismatches (i.e., determine those places where the surface ocean and atmosphere heat fluxes did not match). This diagnosed flux field could then be added into the coupled

model run as a correction field, in essence translating the ocean heat transport field implied by the observed T and S into the atmospheric heat transport field of the equilibrated coupled model. However, a significant drawback of such schemes is that the future evolution of the atmosphere would likely be affected by these fictitious heat fluxes, casting doubt on the results of the anthropogenic forcing scenarios.

b. The anomaly coupling scheme

To address these issues, the pilot-ACPI project ended up using an anomaly coupling scheme, which works as follows. The heat transport in year 1995, in both the model and observations, can be written as:

$$H_{\rm obs}^{1995} = H_{\rm obs}^{1870} + \Delta H_{\rm obs} \tag{1}$$

$$H_{\rm model}^{1995} = H_{\rm model}^{1870} + \Delta H_{\rm model} \tag{2}$$

where the ocean heat transport anomaly, ΔH, is the change in ocean heat transport due to anthropogenic forcing over the period 1870 to 1995. The utility of the anomaly coupling method arises from the observation that $H^{1870} \gg \Delta H$; i.e., anthropogenic perturbations are only a small part of the mean ocean heat transport[1]. Estimating the terms from the PCM's historical runs, and expressing them as RMS values of the surface heat flux field, H^{1870} $\sim$60-80 W/m^2, while ΔH $\sim$2-4 W/m^2. This motivates approximating the model's heat transport as:

$$H_{\rm model}^{1995} \approx H_{\rm model}^{1870} + \Delta H_{\rm obs} \tag{3}$$

This approximation may be of substantial benefit because errors in ΔH are likely to be much smaller in magnitude than errors in H^{1870}, resulting in smaller model drift needed to correct those errors. In essence, this technique allows the (large) *climatological* heat fluxes from the coupled model's ocean and atmosphere to balance each other, while the (much smaller) *anomalous* heat fluxes due to anthropogenic forcing are directly inserted into the model from the observations. Potentially, this can reduce problems with surface heat flux

[1]This would not be true if anthropogenic forcing resulted in the collapse of the thermohaline circulation.

mismatches by an order of magnitude, with a corresponding reduction the the rate of model drift.

In practice, given that $H(\vec{\mathbf{x}}, t)$ is assumed exclusively a function of T and S, we estimate $\Delta H_{\rm obs}$ (the change in ocean heat transport from 1870 to 1995) by using $\Delta T_{\rm obs}$ and $\Delta S_{\rm obs}$, the changes in T and S from 1870 to 1995. Unfortunately, these fields are not known, since the assimilation data period covers only the relatively brief period of 1992-1997[2]. Therefore, another approximation is required to obtain the proper anomaly fields $\Delta T_{\rm obs}$ and $\Delta S_{\rm obs}$ given the absolute fields T and S.

To obtain $\Delta T_{\rm obs}$ and $\Delta S_{\rm obs}$, we make the assumption that the majority of the anthropogenic forcing signal can be obtained by taking the difference between the assimilated T, S fields averaged over 1995-1997 and the Levitus (1994) climatological T, S fields. Part of the motivation for this is that the assimilation procedure starts with the Levitus fields at the beginning of the run, before incorporating recent observations; thus, the assimilation procedure results in forced departures from Levitus climatology.

This assumption may introduce errors to the extent that the Levitus climatology does not represent the state of the ocean in 1870. The actual time that the Levitus climatology represents is uncertain, and perhaps ill-defined given the continuously increasing anthropogenic forcing over the modern time period. Fig. 2 shows the fraction of ocean volume (to 3000m) sampled by Levitus as a function of time; a simple weighted average of the data suggests an average time around 1970. In lieu of direct oceanic measurements, we estimate the amount of ocean heating from 1870 to 1970 from the record of global surface temperatures (Fig. 3; Jones et al. 1999). These show that about 1/3 of the warming experienced from 1870 to 2000 had already happened by 1970. Therefore, we proceed with estimating $\Delta T_{\rm obs}$ and $\Delta S_{\rm obs}$ as the difference between T, S and the Levitus climatologies, with the caveat that this may introduce an error by underestimating the strength of the ocean heating by up to one-third.

Approximating the ocean's heat transport as in Eq. 3 is not guaranteed to eliminate the

[2]The assimilation is being extended to cover the period 1950-2000.

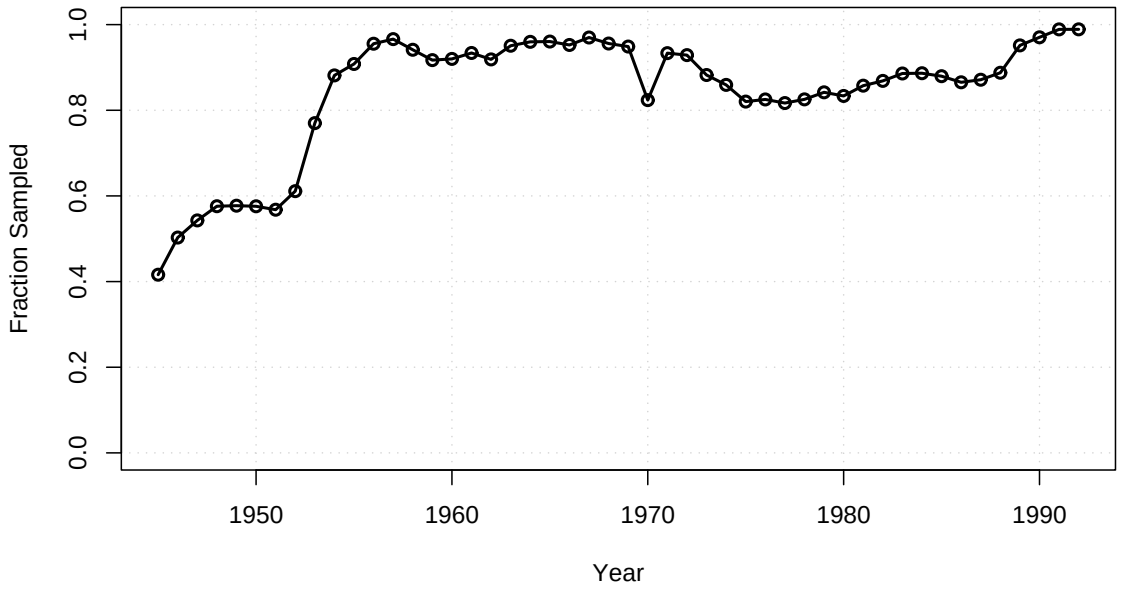

Figure 2: Fraction of the world ocean volume to 3000m sampled by the Levitus data set, as a function of time.

problem of model temperature drift. Although the anomaly coupling method mandates that the model's *climatological* heat transports will be in balance, there is no such assurance for the anomalous heat transports, which are substituted into the model from observations. Furthermore, it is the anomalous heat transports that are important, since they represent the anthropogenic forcing signal. An order-one error in this field would (by definition) represent as much drift as the signal of interest. Therefore, a method must be found for assessing how similar the model's anomalous heat transport is to the observations.

c. Evaluating the assimilated data

As previously, the similarity between the model and observed anomalous heat transports will be evaluated by comparing the anomalous T fields[3]. This will be done with the projection, $\mathcal{P}$, defined as:

$$\mathcal{P} = \frac{d \cdot p}{p \cdot p} \tag{4}$$

[3]This assumes that the observed anomalous T and velocity fields acting on the model's mean fields result in the correct heat transport anomalies.

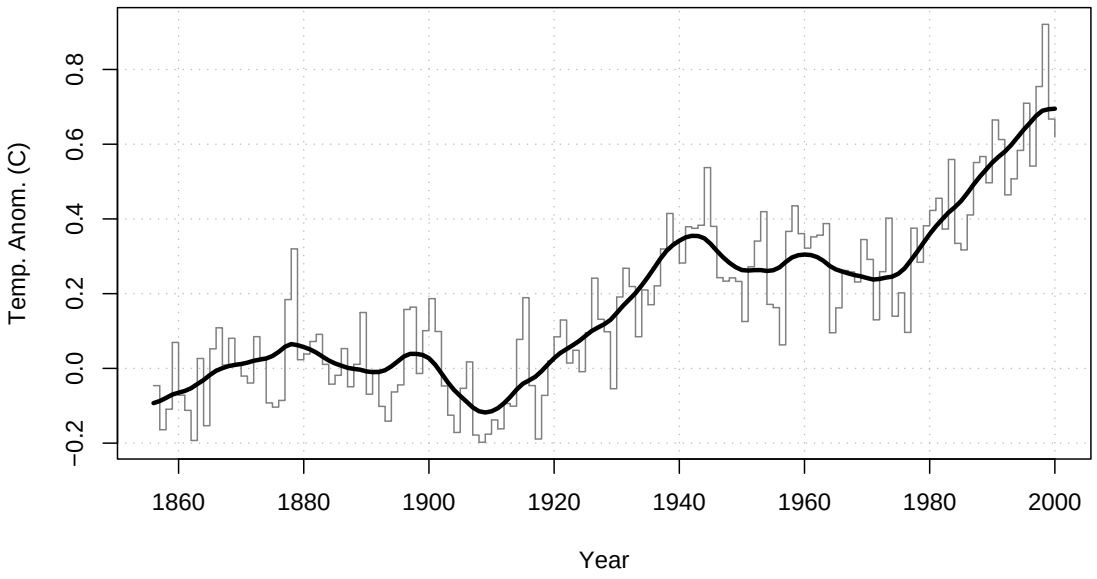

Figure 3: Annual global average surface temperature anomalies (C) with respect to the 1860-1900 average. Data is from P. Jones, UEA (downloaded from http://www.cru.uea.ac.uk/cru/data/temperature/).

where $d(\vec{\mathbf{x}})$ is the data and $p(\vec{\mathbf{x}})$ is a pattern of interest. The projection is closely related to the pattern correlation of d and p:

$$\mathcal{C} = \frac{d \cdot p}{(d \cdot d)^{1/2}(p \cdot p)^{1/2}} \tag{5}$$

but has a normalization that preserves information on the relative strength of d and p as well as their geographical similarity. So, for example, if d looks exactly like p (in both pattern and strength) then $\mathcal{P} = 1$; if d looks geographically similar to p but is twice as strong, $\mathcal{P} = 2$; if d is similar to p but half as strong, $\mathcal{P} = 1/2$; and so on.

The target pattern p used for the projection was the ocean T anomaly field below 250 m, averaged over three ensemble members of the coupled model's business as usual (BAU) runs, and averaged over years 2090 to 2099. Only results below 250 m were considered to reduce the influence of interannual and interdecadal variability (such as ENSO and the north Pacific oscillation), which are strongest in the upper 250 m of the water column and were not of direct interest in this project. The results of the projection are shown in Fig. 4. The projection is calculated for each decade of the three BAU runs (from the 2000's to the 2090's) as well as for five historical runs (covering the 1870's to the 1990's). Note that $\mathcal{P} \approx 1$ for each of the BAU runs by year 2100, in accord with how the target pattern was formed. Fig. 4 shows that by year 2000, the ocean has experienced $\sim$17% of the warming that will be accomplished by 2100.

Also illustrated in Fig. 4 (circles) are the results from projecting the T anomaly fields from the assimilation run onto the target pattern, by year. (Only retaining temperatures below 250 m prevents the strong El Nino year of 1997 from showing up as an anomaly.) It can be seen that the assimilation results are in reasonable agreement with the model results, although on the low side if averaged over all the years (this is in accord with the estimate above that the assimilated results may be up to $\sim$30% too low since the anomalies are not with respect to pre-industrial conditions). Nevertheless, Fig. 4 motivates using the average T,S anomaly fields of the last three years of the assimilation run as the proper anomaly fields to add to the model climatology in forming the initial condition, since the projection values indicate that the assimilated fields have about the proper pattern of temperature

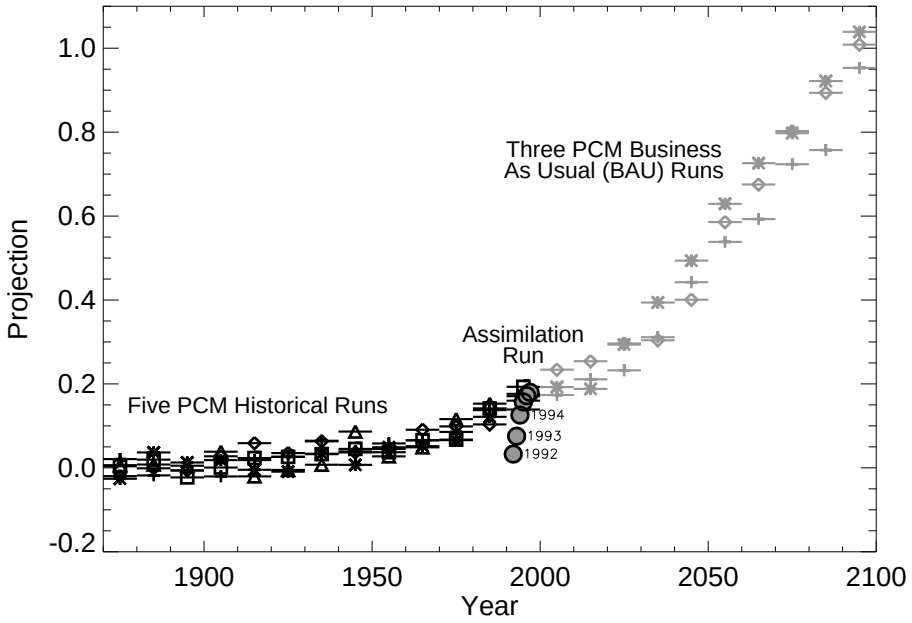

Figure 4: Projection of the model's ocean warming pattern (below 250 meters) in year 2100 onto the five model historical runs and three model business as usual (BAU) runs. The historical and BAU results are averaged by decade, as indicated by the horizontal bars. Also shown (circles) are the projections of the assimilated data onto the same target pattern; the first three years of the assimilation run are labeled by year.

anomalies, in about the proper strength, as compared to the model. This agreement with the model should result in minimal model drift, since with this initial condition both the climatological and anomalous oceanic heat transport fields will be in accord with what the atmospheric model simulates for 1995.

The actual warming patterns (i.e., temperature anomaly below 250 m) for the assimilated data in year 1997 and the model averaged over the 2090's are shown in Fig. 5. The data have been spatially filtered to retain features gyre-scale and larger, as we do not expect the model to capture the details of smaller oceanic features. The PCM experiences most of the warming in the North Atlantic and along the Antarctic circumpolar current (ACC); there is a relative minimum of warming in the central North Pacific. The assimilated data also has most of its warming in the North Atlantic (but farther northeast than in PCM) and the ACC; a band of smaller values is seen in the Pacific, as in PCM, but also extends into the southeast Pacific. The pattern correlation between the two fields is 0.56, which is significant at the 95% level (based on the 12 degrees of freedom left after the spatial filtering). Note that the PCM field is smoother at least partly because of the greater averaging done (across 10 years and 3 ensemble members). This averaging is desirable, as it reduces high frequency variability not of interest here, but is not possible with the short, unique realization of the assimilated data set.

d. Final model drift

The degree of drift still needs to be tested, because of the various approximations and inferences outlined above. This was done using a 50-year control run with the assimilated initial conditions but anthropogenic forcing held fixed at 1995 values. The results are shown in Fig. 6. The heavy solid line is the global average surface temperature for the control run with assimilated initial conditions. Also shown is the ensemble average global surface temperature for the five BAU runs (light line with circles), along with +/- 2 standard deviations (dotted lines). The temperature drift in the control run is about 0.2 C in 50 years. This compares favorably to the forced response of 1.0 C over 50 years, as estimated from the BAU runs. Thus, the assimilation technique reduces the problem of drift to the point

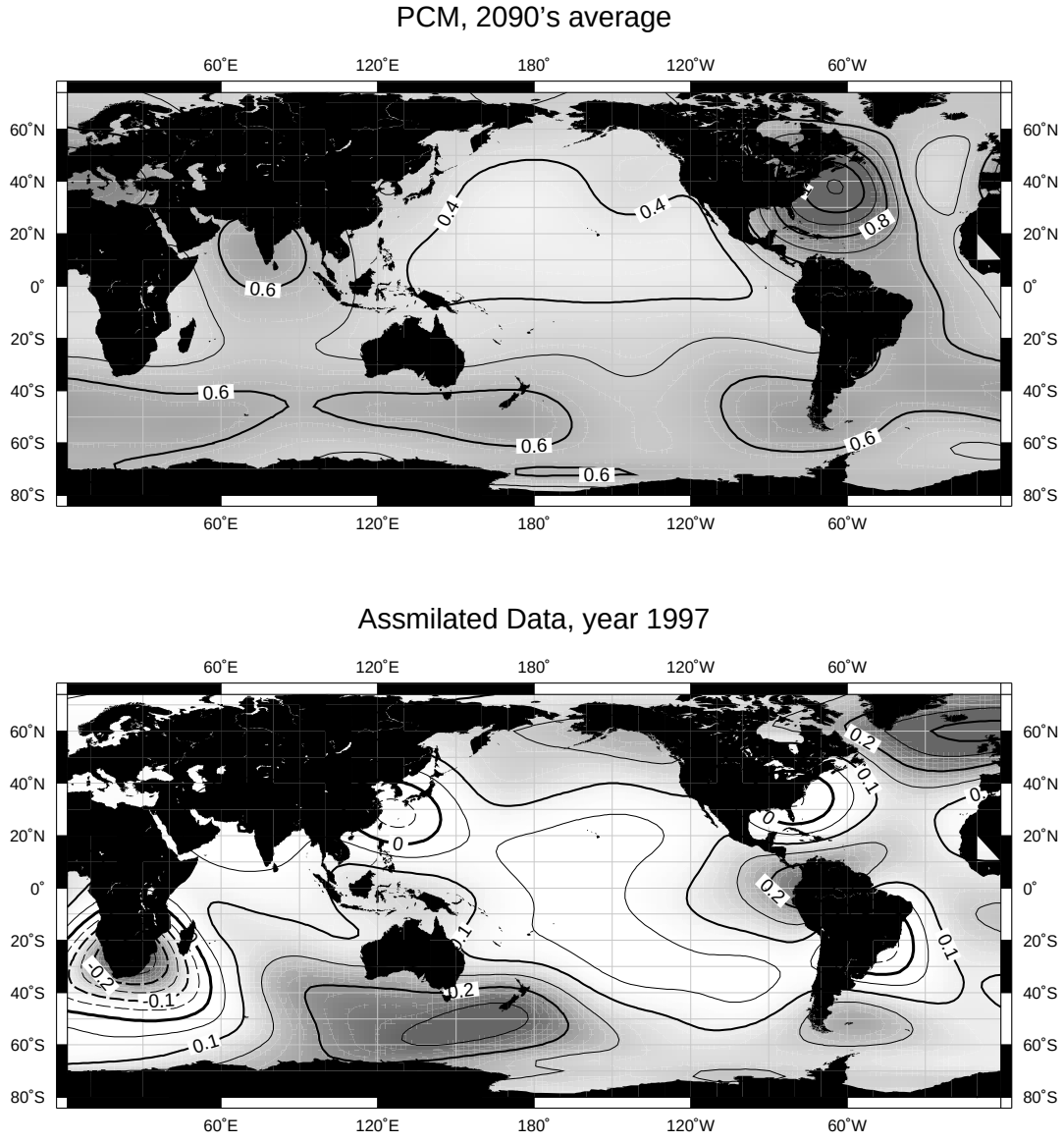

Figure 5: Temperature anomaly (C) below 250 m. Top: model field, decade of the 2090's. Bottom: assimilated data field, year 1997.

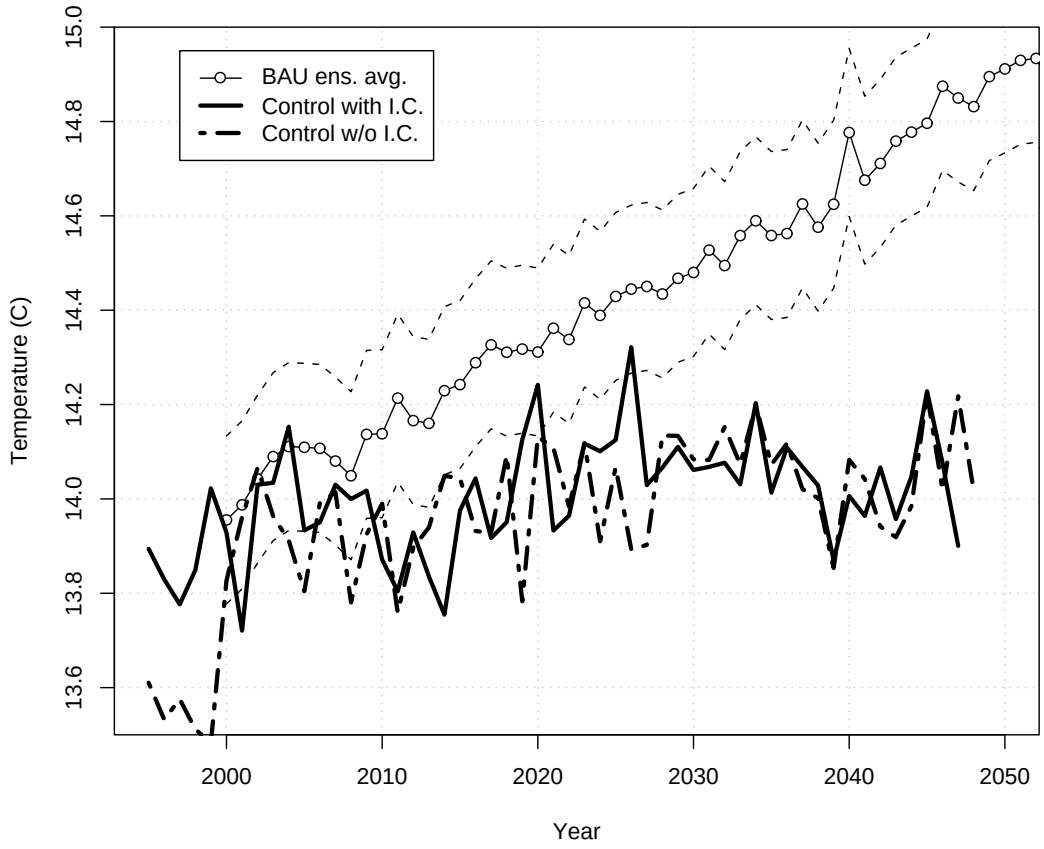

Figure 6: Global-average surface temperature (C). Light line with circles: the ensemble average for the five BAU runs, along with +/- 2 standard deviations of the ensemble spread (light dotted lines). Solid heavy line: the control run with assimilated initial conditions imposed. Broken heavy line: the control run without any assimilated initial conditions imposed.

where it is no more than 1 part in 5 of the forced signal. Additionally, by year 2050 the distribution of values found in the BAU runs is well separated from the variability found in the control run.

There is reason to think the drift attributable to the initial conditions might actually be much smaller than this. The climate state in 1995 is not in equilibrium, since the anthropogenic forcing in 1995 is increasing while the adjustment time of the climate system is on the order of decades. Therefore, one would expect the model to drift even if *no* anomalies were imposed in the initial condition. This was tested in a separate run, illustrated by the heavy broken line in Fig. 6, which was started with pre-industrial model climatology without any assimilated T and S anomalies. As expected, starting with 1995 forcing conditions but pre-industrial model climatology results in a fast ($\sim$5 yrs) initial temperature discontinuity as the surface ocean comes into adjustment with the forcing, but thereafter the drift in the run without assimilated initial conditions is virtually the same as that found using the initial conditions. The initial conditions are thus fulfilling their role of capturing the changes in ocean state between 1870 and 1995 (therefore minimizing the initial shock), but apparently contribute little to model drift in and of themselves.

We conclude that the anomaly coupling method satisfies the desired criterion of initializing with an observationally-based estimate of the climate state in the late 20th century, while still imposing minimal drift on the model solution.

5. Initializing to a neutral ENSO state

The assimilated data covered the period 1992-1997. As noted in Fig. 4, the last three years of this period provide the best fit between the model and observed deep heating fields. However, 1997 was also the year during which an extremely strong El Nino developed. It was deemed inappropriate to include these unusual conditions in the model initialization (although the actual effect of doing so appears unimportant based on the ensemble of BAU runs, which were started from various initial conditions of the control run).

To remove the ENSO and other high frequency (surface trapped) variability, thereby initializing the model to neutral conditions, a vertical weighting scheme was applied to

the assimilated temperature anomalies before they were added to the model climatology. The objective of the scheme is to preserve the heat content anomaly associated with the anthropogenic warming, but damp the heat content anomalies associated with ENSO and other interannual to decadal variability. Accordingly, temperature anomalies below 250 m were not altered (to preserve the anthropogenic warming signal accumulated from 1870 to 1997), while values above 250 m were ramped to zero at the surface.

An estimate of the effect this weighting has on the anthropogenic heat content signal is shown in Fig. 7. In the left panel, the heavy line is the ensemble average of five PCM historical integrations, showing the vertical profile of ocean temperature anomalies that arise from anthropogenic forcing over the period 1870 to 1995 (averaged over the globe). The signal is largest at the surface but still has significant expression even down to 3000 m. Applying the weighting profile (right panel of Fig. 7) to the temperatures results in the profile shown as the thin line with circles. This profile has 18% less heat content than the original vertical temperature profile, i.e., 82% of the anthropogenic heat content signal is retained by this weighting. Note that the profile of *anomalies* is 0.15 C colder at the surface than at 200 m. This would result in an unstable density profile if the anomalies were not added back onto the mean background conditions, which have a far greater stable stratification ($>$ 9 C over the top 200 m) that prevents instability from occurring.

The vertical temperature profile of the ENSO signal is more top-trapped than the anthropogenic signal. This can be determined by taking the leading EOF (not shown) of the White (1995) three-dimensional temperature XBT-based data set, horizontally averaged and high-pass filtered to remove periods longer than 7 yrs/cycle (i.e., retaining ENSO periods but discarding the secular anthropogenic signal). The peak in the response is at 40 m depth; 87% of ENSO's r.m.s. heat content signal is above 250 m. Applying the same weighting profile (Fig. 7, right panel) removes 51% of the heat content signal due to ENSO (compared to 18% of the heat content signal due to the anthropogenic forcing). While not perfect, this scheme gives a reasonable compromise between removing the ENSO signal, retaining the anthropogenic signal, and simplicity.

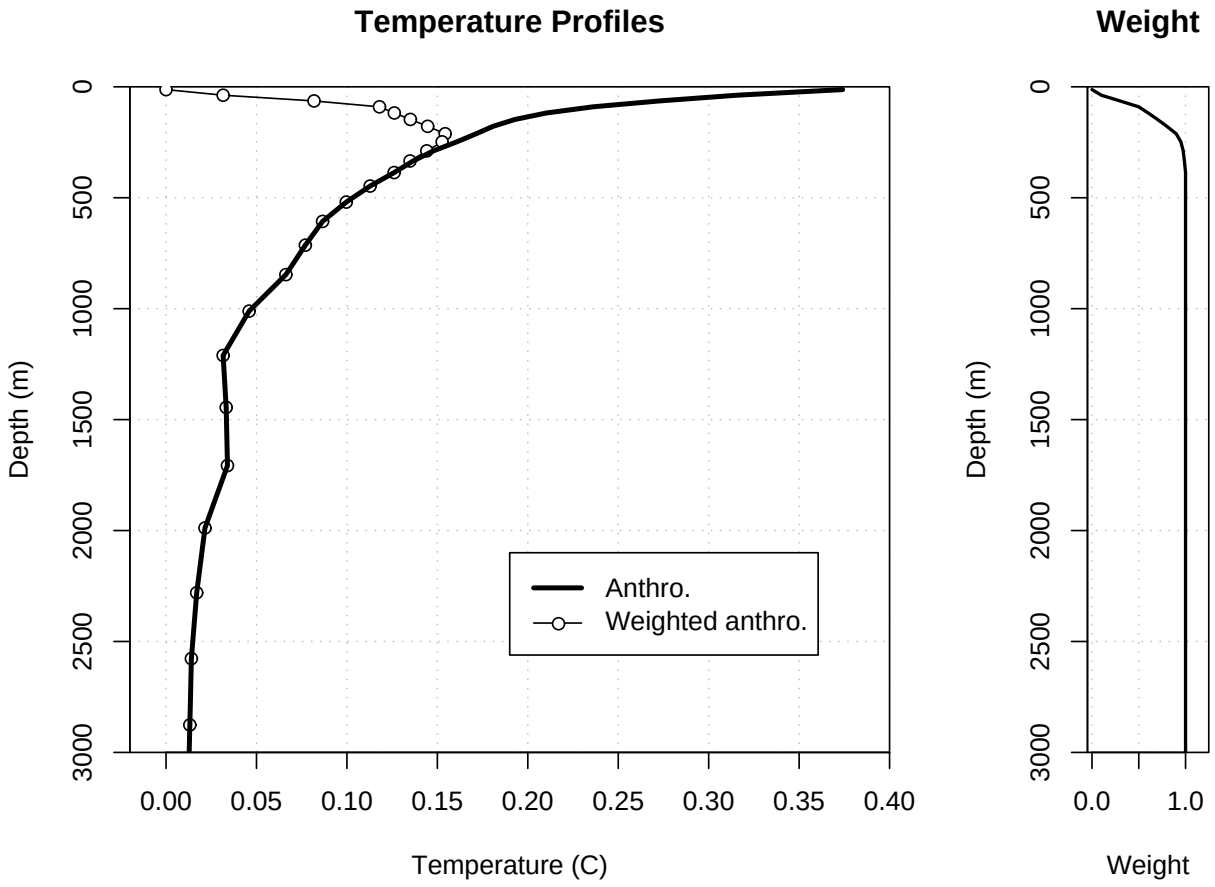

Figure 7: Left: vertical temperature profiles (C) for the model-estimated anthropogenic signal as of 1995 (heavy solid line), and the anthropogenic signal after weighting with the profile shown in the right hand panel (light line with circles).

It should be noted that initializing the model to near-neutral ENSO conditions in the ocean does not prevent the subsequent development of any non-linear interactions between anthropogenic forcing and ENSO (or other interannual to decadal variability). This is important, as is well known that seasonal rainfall and temperatures over the western U.S. are affected by ENSO (e.g., Cayan et al. 1999) and the north Pacific oscillation (NPO; e.g., Latif and Barnett 1996). These effects will be present in the pilot-ACPI predictions, and it is entirely possible that one manifestation of anthropogenic forcing will be a change in the frequency or amplitude of ENSO (e.g., Cane et al. 1997, Timmermann et al. 1999, Meehl and Washington 1996). This could be one of the dynamical mechanisms by which the average climate in year 2050 is changed, and so its inclusion here is important.

6. Assimilated versus spun-up initial conditions

There are two reasons for initializing the model from observations rather than using a long spinup run from pre-industrial conditions: 1) to save computer time; 2) to obtain an initial condition that gives a more accurate simulation of future climate. The anomaly coupling technique certainly saves computer time, which leaves us with the question of whether it leads to more accurate predictions. Although this will not be known for some decades, we can at least evaluate whether the assimilated initial conditions made any difference. This evaluation is possible because there already exists a set of "standard" PCM runs that start with pre-industrial conditions and integrate forward past year 2050 with BAU forcing.

A problem with evaluating whether the assimilated initial condition made any difference is the small sample size: the pilot ACPI ensembles have only three members. To address this, we used the non-parametric technique devised by Preisendorfer and Barnett (1983), which was constructed specifically for this type of problem. Outputs are a 'SITES' and 'SPRED' statistic (described below).

Briefly, for every variable (e.g., global temperature) we have two data sets, each with n ensemble members and p spatial points. In our case, the two data sets are the pilot ACPI runs and the standard PCM BAU runs, each with 3 ensemble members. The SITES statistic

gives the distance between the centroids of the two swarms of n points in the p-dimensional state space. As such, it takes into account differences in both the r.m.s. means of the data (the lengths of the state vectors), and their geographical patterns (the directions of the state vectors). The SPRED statistic is an indicator of the intra-ensemble scatter. These statistics can be compared to estimates of the expected distributions of SITES and SPRED obtained by the 'PPP' random subsetting procedure (Preisendorfer and Barnett 1983; the idea is similar to the bootstrap scheme of Efron 1993). The end result shows how likely is the actual grouping of ensemble members into data sets. If the grouping appears to be random, then it can be inferred (in our particular case) that there is no systematic difference between runs with assimilated or spun-up initial conditions. Other possible outcomes are that the ensembles are unusually different, which would suggest that the assimilation had a significant effect, or that the ensembles are improbably similar, which would suggest that the initialization technique failed to modify the initial T, S fields in the first place.

Examples of the SITES statistic for two test cases, intended to illustrate the nature of the statistic, are shown in Fig. 8. In this and later plots, three year chunks of the data are averaged together to reduce year-to-year noise. In the top panel, annually averaged surface temperature (TS) over North America from two different 3-member ensembles of PCM historical runs are compared. This case is useful because it illustrates what to expect when only natural variability is acting. The X axis indicates the year of comparison. In this case, the statistical properties of TS in set 1 are being compared to the same field in set 2, *at the same year*. For example, at X=1940, we see that Y$\sim$60, which indicates that the actual SITES statistic for this case was in the 60th percentile of the estimated distribution. Thus, the actual value of the statistic was likely to occur by chance, and we cannot confidently assert that there is any difference between runs in set 1 and 2. For small percentiles ($<$10), runs in set 1 and 2 are more similar to each other than would be expected by chance given the natural variability; for large percentiles ($>$90), runs in set 1 and 2 are more different than expected by chance. The results in the top panel show the historical PCM ensembles are statistically indistinguishible from each other when sampled at the same year. In the

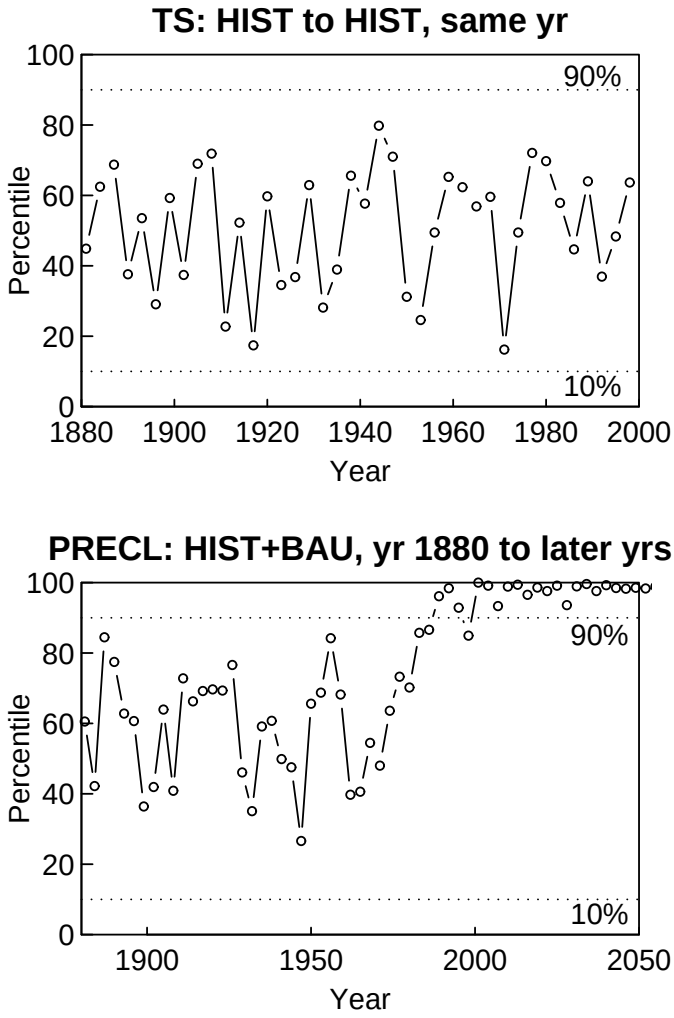

Figure 8: SITES statistic for two test cases. Top: surface temperature (TS) over North America from two separate 3-member ensembles, compared at the same year; no difference is expected beyond that arising from natural variability. Bottom: large scale precipitation (PRECL) over the globe, comparing year 1880 to later years. By 2000, a significant difference is found. See text for further details.

bottom panel, globally averaged large-scale precipitation (PRECL) fields are compared for a thee-member ensemble of historical runs (1880-1999) extended by BAU runs (2000-2050). In this case, the fields at year 1880 are being compared to fields at progressively later years. The SITES statistic shows that by year 2000, the global precipitation field has become significantly different from that found in 1880. This case is useful because it illustrates what to expect when the test fields are different.

Figure 9 shows the SITES statistic comparing the pilot ACPI runs to the standard PCM BAU runs over North America. If the different initial conditions made a difference to the climate, then this statistic would start significantly high (>90), then drop to average values after some physically-dictated time lag. What Fig. 9 actually shows is that the varying initial condition made no difference, even at short time lapses, to any variable. For completeness, we also checked the northern hemisphere and global fields, and the SPRED (intra-ensemble variance) statistic as well as the SITES statistic. In no case did the initial conditions make any difference, except to the accumulated snow depth field atop Antarctica, which was not reset to a consistent value at the start of all the runs (this is irrelevant to the ocean initialization procedure we are examining).

It is worth carefully considering this result in light of section 4, which showed that the heat content anomaly obtained from the PCM spinup runs is similar in pattern and magnitude to the assimilated initial conditions (Fig. 4). It is likely that the null effect of assimilated initial conditions is another reflection of the similarity between PCM and the assimilated data. If so, then a model less like the observations might benefit substantially by using the assimilated initial conditions. In any event, the correct conclusion is *not* that that the details of the 1995 climate make no difference to later years, but rather that substituting the assimilated initial conditions into PCM in place of the spinup conditions makes no difference to later climate. It cannot be ruled out that this is simply because PCM simulates the initial condition rather well.

7. Summary and conclusions

The objective of the pilot-ACPI project was to produce “end-to-end” forecasts of hy-

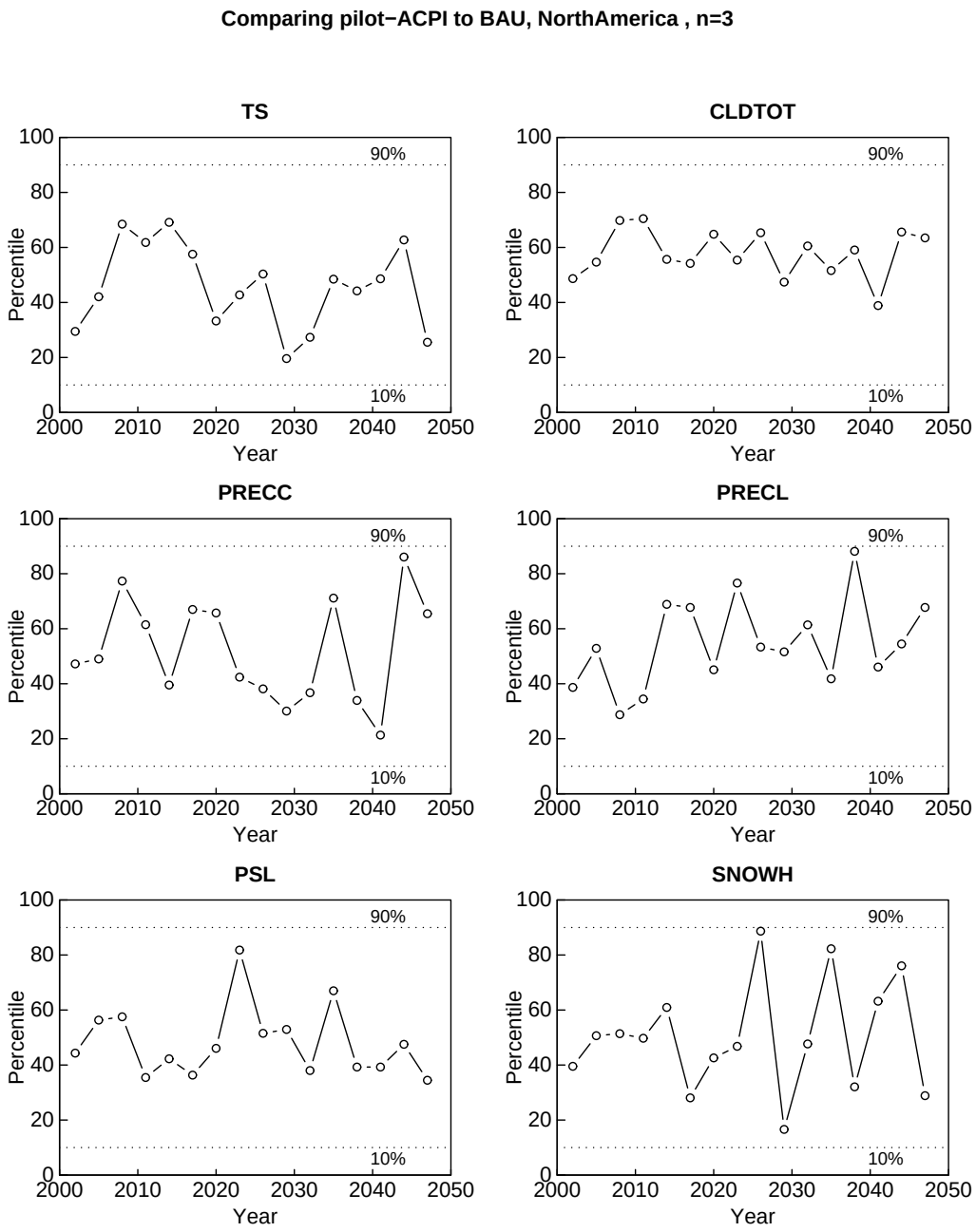

Figure 9: SITES statistic comparing the pilot ACPI run to the standard PCM BAU runs. Variables compared are: TS=surface temperature; CLDTOT=cloud fraction; PRECC=convective precipitation; PRECL=large scale precipitation; PSL=sea level pressure; SNOWH=snow depth. Values over North America were included. See text for further details.

drological processes over the western U.S. in the year 2050. This involved initializing the coupled ocean-atmosphere model to the current observed climate state, running the coupled model to the year 2050 and beyond with projected anthropogenic forcing, and downscaling the results to the hydrological impact over the western U.S. This note describes the techniques used to accomplish the first element (initializing the coupled model to observed conditions) and an evaluation of the difference this made.

There were three main problems encountered: the lack of comprehensive three-dimensional temperature and salinity observations to initialize to, the likelihood of model drift arising from inserting observed conditions into a numerical model, and the initialization to a short data set that included an unusually strong El Nino year (1997). The first problem was solved by using an assimilated data set from a full adjoint model. The second problem was solved by using an anomaly coupling technique, such that the observed heat transport anomalies associated with the anthropogenic signal were added onto the base model climatology. It was shown that this technique worked because the model and observed patterns of anomalous temperature were similar in both strength and magnitude. The last problem was solved by ramping temperature anomalies to zero near the surface (above 250 m), so that the main part of the anthropogenic heat content signal was retained while the higher-frequency signals of interest (such as ENSO) were damped towards neutral conditions.

Comparing the predictions of the pilot ACPI runs to standard (spun up from pre-industrial conditions) PCM BAU runs, it was found that the assimilated initial conditions made no systematic difference. This is likely another reflection of the similarity between the model and observed patterns of anomalous temperature; switching from the spinup to the assimilated conditions is a relatively small change. This might be different in a model that had a worse representation of the anomalous ocean heat content in the late 20th century.

This work leaves unanswered why the model spinup and assimilated initial conditions are so similar. It might be that both the model and the assimilation are skillful in predicting this field, in which case their similarity is testament to the good quality of the results. It could also be because both are based on modern general circulation models (although

different ones), which might have similar systematic errors. Independent analysis of model versus observed heat content fields (Levitus et al. 2001, Barnett et al. 2001) suggest that models can, in fact, skillfully capture this field. However, a detailed comparison of the assimilated versus observed data remains to be done. It is hoped that this issue will be addressed in a full ACPI project.

8. Acknowledgments

This work was supported by the Department of Energy under grant DE-FG03-98ER62505. Most of the computations for the work described here were done under the auspices of the National Partnership for Advanced Computer Infrastructure (NPACI) at the San Diego Supercomputer Center, with the tremendous help of Peter Arzberger and Giridhar Chukkpalli. The rest were done at Oak Ridge National Laboratory, with the help of John Drake. These contributions are gratefully acknowledged.

REFERENCES

Adcroft, A., C. Hill, J. Marshall, 1997: Representation of topography by shaved cells in a height coordinate ocean model. *Mon. Wea. Rev.*, v. **125** p. 2293-315.

Barnett, T. P., D. W. Pierce, R. Schnur, 2001: Detection of anthropogenic climate change in the world's oceans. *Science*, v. **292** p. 270-274.

Cane, M. A., A. C. Clement, A. Kaplan, Y. Kushnir, D. Pozdnyakov, R. Seager, S. E. Zebiak, R. Murtugudde, 1997: Twentieth-century sea surface temperature trends. *Science*, v. **275** p. 957-60.

Cayan, D. R., K. T. Redmond, L. G. Riddle, 1999: ENSO and hydrologic extremes in the Western United States. *J. Climate*, v. **12** p. 2881-2893.

Dukowicz, J. K., R. D. Smith, 1994: Implicit free-surface method for the Bryan-Cox-Semtner ocean model. *J. Geophys. Res.*, v. **99** p. 7991-8014.

Efron, B., 1993: An introduction to the bootstrap. *(null)*, p. 436-0.

Hasselmann, K., R. Sausen, E. Maier-Reimer, R. Voss, 1993: On the cold start problem in transient simulations with coupled atmosphere-ocean models. *Clim. Dyn.*, v. **9** p. 53-61.

Hunke, E. C., J. K. Dukowicz, 1997: An elastic-viscous-plastic model for sea ice dynamics. *J. Phys. Oceanogr.*, v. **27** p. 1849-67.

Jones, P. D., M. New, D. E. Parker, S. Martin, I. G. Rigor, 1999: Surface air temperature and its changes over the past 150 years. *Rev. of Geophysics*, v. **37** p. 173-199.

Kiehl, J. T., J. J. Hack, G. B. Bonan, B. A. Boville, D. J. Williamson, P. J. Rasch, 1998: The National Center for Atmospheric Research Community Climate Model: CCM3. *J. Climate*, v. **11** p. 1131-1149.

Latif, M., T. P. Barnett, 1996: Decadal Climate Variability over the North Pacific and North America: Dynamics and Predictability. *J. Climate*, v. **9** p. 2407-2423.

Levitus, S., 1994: World ocean atlas 1994. U.S. Dept. of Commerce, National Oceanic and Atmospheric Administration, 0 pp.

Levitus, S., J. I. Antonov, T. P. Boyer, 2000: Warming of the world ocean. *Science*, v.

287 p. 2225-2229.

Levitus, S., J. I. Antonov, Delworth Julian Wang, Dixon T. L., Broccoli K. W., A. J., 2001: Anthropogenic warming of Earth's climate system. *Science*, v. **292** p. 267-70.

Marshall, J., C. Hill, L. Perelman, A. Adcroft, 1997a: Hydrostatic, quasi-hydrostatic, and nonhydrostatic ocean modeling. *J. Geophys. Res.*, v. **102** p. 5733-52.

Marshall, J., A. Adcroft, C. Hill, L. Perelman, C. Heisey, 1997b: A finite-volume, incompressible Navier Stokes model for studies of the ocean on parallel computers. *J. Geophys. Res.*, v. **102** p. 5753-66.

Meehl, G. A., W. M. Washington, 1996: El Nino-like climate change in a model with increased atmospheric CO2 concentrations. *Nature*, v. **382** p. 56-60.

Preisendorfer, R. W., T. P. Barnett, 1983: Numerical model-reality intercomparison tests using small-sample statistics. *J. Atmos. Sci.*, v. **40** p. 1884-1896.

Schneider, E. K., 1996: Flux correction and the simulation of changing climate. *Annales Geophysicae*, v. **14** p. 336-41.

Smith, R. D., J. K. Dukowicz, R. C. Malone, 1992: Parallel ocean general circulation modeling. *Physica D*, v. **60** p. 38-61.

Stammer, D., C. Wunsch, R. Giering, Q. Zhang, J. Marotzke, J. Marshall, C. Hill, 1997: The Global Ocean Circulation Estimated from TOPEX/POSEIDON Altimetry and the MIT General Circulation Model. Technical Report "Report No. 49", Available from MIT Center for Global Change Science, Cambridge, MA 02139 US.

Timmermann, A., J. Oberhuber, A. Bacher, M. Esch, M. Latif, E. Roeckner, 1999: Increased El Nino frequency in a climate model forced by future greenhouse warming. *Nature*, v. **398** p. 694-7.

Washington, W. M., J. W. Weatherly, G. A. Meehl, A. J. Semtner, T. W. Bettge, A. P. Craig, W. G. Strand, J. Arblaster, V. B. Wayland, R. James, Y. Zhang, 2000: Parallel Climate Model (PCM) control and transient simulations. *Climate Dynamics*, v. **16** p. 755-74.

White, W. B., 1995: Network design of a global observing system for gyre-scale upper

ocean temperature variability. *Prog. Oceanogr.*, v. **36** p. 169-217.

Zhang, J., W. D. Hibler, 1997: On an efficient numerical method for modeling sea ice dynamics. *J. Geophys. Res.*, v. **102** p. 8691-702.